

# Signals of a new phase in $\mathcal{N} = 2$ gauge theory with a magnetic field on the three-sphere

---

**Suphakorn Chunlen, Kasper Peeters, Pichet Vanichchaponjaroen  
and Marija Zamaklar**

*Department of Mathematical Sciences,  
Durham University,  
South Road,  
Durham DH1 3LE,  
United Kingdom.*

*E-mail:* [suphakorn.chunlen@durham.ac.uk](mailto:suphakorn.chunlen@durham.ac.uk),  
[kasper.peeters@durham.ac.uk](mailto:kasper.peeters@durham.ac.uk),  
[pichet.vanichchaponjaroen@durham.ac.uk](mailto:pichet.vanichchaponjaroen@durham.ac.uk),  
[marija.zamaklar@durham.ac.uk](mailto:marija.zamaklar@durham.ac.uk)

**ABSTRACT:** We study the effect of a magnetic field on  $\mathcal{N} = 2$  super-Yang-Mills on  $S^3$  at strong coupling using the gauge/gravity correspondence. As in previous work that dealt with the theory in infinite volume, we find that increasing the magnetic field pushes the system into the confined phase. However, we in addition also find that, within the class of configurations with the same symmetry as those which describe the ground state at vanishing magnetic field, a mass gap appears in the spectrum. This suggests the existence of a new phase with so far unexplored symmetry structure. We provide suggestions for the physical properties of this phase.

---

## Contents

<b>1</b>	<b>Introduction</b>	<b>1</b>
<b>2</b>	<b>Review of global <math>\text{AdS}_5 \times S^5</math> and D7-brane phases</b>	<b>3</b>
<b>3</b>	<b>Introducing a magnetic field into the system</b>	<b>5</b>
3.1	Equations of motion and the ansatz	5
<b>4</b>	<b>Solving the equations of motion</b>	<b>9</b>
4.1	Comments on the numerical analysis	15
<b>5</b>	<b>Understanding the mass gap and behaviour of ball branes</b>	<b>16</b>
5.1	Appearance of the gap: disappearance of critical branes	17
5.2	Behaviour of the equatorial brane and maximal value of magnetic field	18
<b>6</b>	<b>Fluctuation analysis and investigation of the gap</b>	<b>19</b>
6.1	Stability analysis of the branes	20
6.2	Investigating the gap	25

---

## 1 Introduction

While a lot of effort has been invested in understanding the properties of gauge theories in infinite volumes using holography, much less attention has been spent so far on understanding holographic duals in compact spaces. In this paper we look at the effect of a magnetic field on gauge theory in compact space in the simplest setting in which the dual is  $\text{AdS}_5 \times S^5$  supplemented with probe D7-branes.

String theory in global  $\text{AdS}_5 \times S^5$  space is believed to be dual to  $\mathcal{N} = 4$  super-Yang-Mills theory at zero temperature, which lives on the boundary of this space, an  $S^3 \times \mathbb{R}$ . Adding probe D7-branes in this geometry corresponds to adding flavour hypermultiplets to the system. In the absence of a chemical potential or magnetic field, the asymptotic position of the probe branes is an arbitrary parameter related to the bare quark mass. It was first observed in [1] and later investigated in detail in [2] that at zero temperature, the probe brane undergoes a third order, topology changing phase transition at some value of the bare quark mass. There are thus two phases, corresponding to what [3]

calls *ball* branes and *Minkowski* branes. Ball branes are those branes that extend all the way to the origin of the AdS space, where an  $S^3 \in \text{AdS}_5$  wrapped by the probe brane shrinks to zero size. When the bare quark mass is increased above some critical value, Minkowski branes appear. The Minkowski branes do not reach the AdS origin. At a finite distance from the AdS origin, the  $S^3 \in S^5$  wrapped by the probe brane shrinks to zero size. See figure 1 below for a schematic summary. These two types of branes obviously have different topologies, and their existence is specific for the *global*  $\text{AdS}_5 \times S^5$  space, as in the infinite volume or Poincaré limit, only ball branes exist.

The physical reason for the existence of this phase transition at zero temperature is the non-vanishing Casimir energy of the field theory on the compact space. The compact sphere on which the theory lives introduces a new scale in the problem, which is the size of the sphere. Therefore, all quantities, including the bare quark mass, are now expressed in term of this scale. One way of thinking about the phase transition from Minkowski branes to ball branes [2] is that instead of decreasing the bare quark mass, one keeps the quark mass of the probe fixed while squeezing the system into an ever smaller volume. When the radius of the sphere reaches the critical value  $R_3^* = 0.18\sqrt{\lambda}/m_q$  [2], the system undergoes a phase transition, in which “mesonic” particles “fall apart”, since their zero point energy due their confinement to the finite volume becomes larger than their binding energy.

In a previous paper [4] we have looked at the effects of an isospin chemical potential in this compact geometry, using holographic methods. We have found that this system exhibits an instability for sufficiently large values of the chemical potential. In contrast to other related models, the first excitation to condense is not a vector meson but rather a scalar charged under the global  $SO(4)$  symmetry group. We have also explicitly constructed the new ground state. There is thus reason to suspect that other interesting things could happen due to the finite volume of the system.

In the present paper we would like to understand how the observed phase transition between Minkowski and ball branes changes once a magnetic field is introduced in the system. This situation has previously been analysed by [3] but as we will show explicitly, the magnetic field used in that paper does not satisfy all equations of motion. Because of this, the results of [3] differ significantly from our findings.

We know that a magnetic field in general favours the formation of bound states, so in that sense it has an effect which is opposite from that of the compactness of the space [2, 3]. The question is thus how these two competing effects modify the behaviour of the system. We have found several interesting effects caused by the magnetic field. First, the presence of a magnetic field on the brane worldvolume leads to branes being “repelled” from the origin of the AdS space. A similar effect was observed previously

in the infinite volume, Poincaré limit in [5]. Because the magnetic field enhances the curving of branes away from the origin, it works in favour of ball branes becoming Minkowski. This is indeed what we observe, as for larger values of magnetic field fewer and fewer ball branes remain present in the spectrum. To be precise, they are present in the spectrum for some range of bare quark mass  $0 < m_q < M_{\text{ball}}(B)$ , and the function  $M_{\text{ball}}(B)$  is monotonically decreasing as a function of the magnetic field. When the magnetic field reaches some critical value  $\hat{M}_1$ , all ball branes have disappeared from the spectrum.

A second, somewhat surprising feature caused by the magnetic field is the appearance of a “gap” in the allowed values of the bare quark mass. Even for an infinitesimal value of the magnetic field we observe that ball and Minkowski branes are separated by a range of bare quark masses  $\Delta(B)$  for which none of the two phases are possible. This kind of behaviour was not observed before in the infinite volume Poincaré limit. While we are confident that there are no ball nor Minkowski branes present in the gap, this leaves open the possibility that there are other solutions, with less symmetry, that lead to a brane embedding with mass in the gap. In particular, we will in section 6 present some preliminary results in the direction of constructing an inhomogeneous phase, as a candidate for the “missing” gap branes.

## 2 Review of global $\text{AdS}_5 \times S^5$ and D7-brane phases

In order to set the scene, we will in this section briefly review some properties of the global  $\text{AdS}_5 \times S^5$  space. We will also review the various embeddings of D7-probe branes in these geometries in the absence of external fields, as previously analysed in detail in [1, 2]. The metric of the global  $\text{AdS}_5$  spaces at zero temperature is given by

$$ds^2 = -\frac{u^2}{R^2} \left(1 + \frac{R^2}{4u^2}\right)^2 dt^2 + u^2 \left(1 - \frac{R^2}{4u^2}\right)^2 d\bar{\Omega}_3^2 + \frac{R^2}{u^2} (du^2 + u^2 d\Omega_5^2), \quad (2.1)$$

where

$$d\Omega_5^2 = \frac{d\chi^2}{1 - \chi^2} + \chi^2 d\kappa^2 + (1 - \chi^2) d\Omega_3^2 \quad (2.2)$$

and

$$d\bar{\Omega}_3^2 = d\bar{\theta}^2 + \sin^2 \bar{\theta} d\bar{\phi}^2 + \cos^2 \bar{\theta} d\bar{\psi}^2, \quad d\Omega_3^2 = d\theta^2 + \sin^2 \theta d\phi^2 + \cos^2 \theta d\psi^2. \quad (2.3)$$

Here  $(\bar{\theta}, \bar{\phi}, \bar{\psi})$  parametrise the  $S^3$  in  $\text{AdS}_5$ , and unbarred angular coordinates parametrise the  $S^5$ . In these coordinates the origin of the AdS space is at  $u = R/2$ , while the boundary is an  $S^3$  at  $u \rightarrow \infty$ .

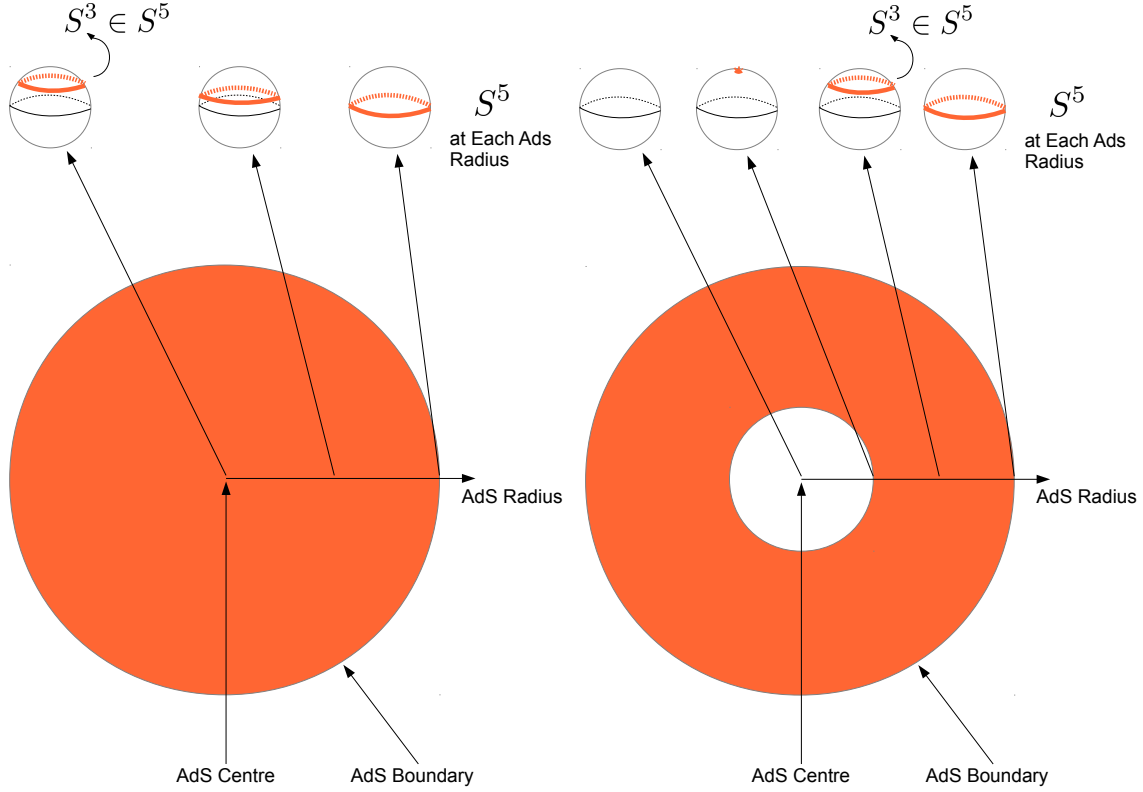


**Figure 1.** Schematic depiction of the two types of D7-brane embeddings in global  $\text{AdS}_5 \times S^5$ . The D7-brane is highlighted in orange. The panel on the left shows a ball embedding, which completely fills the  $\text{AdS}_5$  space. The panel on the right shows a Minkowski embedding. It shrinks on the  $S^5$  at some point before it reaches the origin of  $\text{AdS}_5$ .

In order to reliably do numerical computations it will be useful to switch to compact coordinates for global AdS space, in which the metric reads

$$ds^2 = -\frac{1}{4z^2} (1 + z^2)^2 dt^2 + \frac{R^2}{4z^2} (1 - z^2)^2 d\bar{\Omega}_3^2 + R^2 \frac{dz^2}{z^2} + R^2 d\Omega_5^2. \quad (2.4)$$

The  $z$ -coordinate related to the non-compact  $u$ -coordinate by

$$z = \frac{R}{2u}. \quad (2.5)$$

Let us note that in the  $z$ -coordinate the origin of the AdS space is at  $z = 1$  while the boundary is at  $z = 0$ .

Introducing D7-probe branes in this geometry corresponds, in the holographic language, to adding flavour hypermultiplets to  $\mathcal{N} = 4$  SYM on the sphere  $S^3$ . A study

of various D-brane probes, in particular D7-probe branes, in this geometry was performed in [1, 2]. It was found that at zero (and low) temperature, there are two possible D7-brane embeddings in this dual geometry. The first type of embedding consists of those D7-branes which completely fill the  $\text{AdS}_5$  space. The second type of embedding consists of the D7-branes which wrap a non-maximal  $S^3 \in S^5$  which shrinks along the radial direction of  $\text{AdS}_5$  and collapses before the brane reaches the origin of  $\text{AdS}_5$ . See figure 1 for a schematic comparison.

Within the first series there is one particular embedding in which the brane wraps the equatorial  $S^3 \in S^5$  (i.e. it is a brane with vanishing extrinsic curvature). This system is dual to the  $\mathcal{N} = 2$  SYM theory with massless hypermultiplets. All other embeddings in this class, and all embeddings in the Minkowski class, are dual to a massive hypermultiplet, with a mass related to the distance at which the D7-brane “stops” before the origin of the  $\text{AdS}_5$ <sup>1</sup>. Interestingly, as the “quark” mass is varied a topology changing phase transition occurs [1]. It was further analysed in detail in [2] that this phase transition is actually third order, unlike most of the phase transitions associated to probe branes in holographic duals, which are usually first order.

In the high-temperature phase, the situation is similar to that in infinite volume. One finds that Lorentzian and black hole embeddings exhaust all possibilities. Just as in infinite volume, these correspond to D7-branes that stay outside the horizon or reach the black hole horizon respectively. We will not discuss the high-temperature phase in this paper.

### 3 Introducing a magnetic field into the system

In the previous section we have recalled that empty global  $\text{AdS}_5 \times S^5$  admits two types of D7-branes, depending on the quark mass. The question we want to address now is what happens to the brane embeddings when we introduce an external magnetic field in the direction of the boundary  $S^3$ .

#### 3.1 Equations of motion and the ansatz

The equations of motion for the probe brane with flux follow from the DBI action

$$S = -T_{\text{D7}} \int d^8\sigma \sqrt{-\det(e_{ab} + 2\pi\alpha' F_{ab})}, \quad (3.1)$$

---

<sup>1</sup>A more correct description of the mass is of course given in terms of asymptotic data.

where  $e_{ab} = E_{\mu\nu} \partial_a x^\mu \partial_b x^\nu$  with  $E_{\mu\nu} = G_{\mu\nu} + B_{\mu\nu}$ . We obtain the equations of motion for the embedding function and for the gauge field,

$$\partial_b \left( \sqrt{-\mathcal{E}} \mathcal{E}^{ba} E_{\nu\lambda} \frac{\partial x^\nu}{\partial \sigma^a} \right) + \partial_a \left( \sqrt{-\mathcal{E}} \mathcal{E}^{ba} E_{\lambda\nu} \frac{\partial x^\nu}{\partial \sigma^b} \right) - \sqrt{-\mathcal{E}} \mathcal{E}^{ba} \partial_\lambda E_{\mu\nu} \frac{\partial x^\mu}{\partial \sigma^a} \frac{\partial x^\nu}{\partial \sigma^b} = 0, \quad (3.2)$$

$$\partial_a (\sqrt{-\mathcal{E}} (\mathcal{E}^{ab} - \mathcal{E}^{ba})) = 0, \quad (3.3)$$

where  $\mathcal{E}^{ab}$  and  $\mathcal{E}$  are inverse and determinant of  $\mathcal{E}_{ab} = e_{ab} + 2\pi\alpha' F_{ab}$ , respectively.

The action (3.1) is invariant under the gauge symmetry which involves, on equal footing, the Yang-Mills field strength  $F_{ab}$  on the brane worldvolume and the pull-back of the two form gauge potential  $B_{\mu\nu}$  in the bulk. Hence, having a nontrivial magnetic field strength on the brane worldvolume is equivalent to having a nontrivial  $B$ -flux in the bulk, and would in principle lead to backreaction to the background geometry (even in the probe-brane limit). In order to avoid backreaction of the magnetic field on the D7-brane on the background geometry we will therefore take the  $B$ -field to be pure gauge. We make the following ansatz,

$$B = \frac{1}{2} H'(u) R^2 (\sin^2 \bar{\theta} du d\bar{\phi} + \cos^2 \bar{\theta} du d\bar{\psi}) + H(u) R^2 \sin \bar{\theta} \cos \bar{\theta} (d\bar{\theta} d\bar{\phi} - d\bar{\theta} d\bar{\psi}). \quad (3.4)$$

It is easy to see that the  $B$ -field is indeed pure gauge,  $B = d\Lambda$ , where

$$\Lambda = \frac{1}{2} H(u) R^2 (\sin^2 \bar{\theta} d\bar{\phi} + \cos^2 \bar{\theta} d\bar{\psi}). \quad (3.5)$$

When writing this ansatz we have used the simplest, lowest lying vector spherical harmonic on  $S^3$ , with quantum numbers  $(\bar{l} = 1, \bar{s} = -1)$  (or  $\bar{l} = 1, \bar{s} = 1$ ). While a linear combination of the two would also be pure gauge, it does not satisfy the equations of motion, so in what follows we focus on a single lowest lying spherical harmonic.

We should emphasise that our ansatz differs from the magnetic field studied in [3]. When constructing the ansatz for the magnetic field, their idea was to use the tetrads of the metric on the  $S^3$  (2.3), as these being one-forms would provide a pure gauge magnetic field. While this is true, as we show below, the ansatz of [3] does not satisfy the second equation of motion (3.3) and as such does not describe a physical magnetic field. The ansatz for the magnetic field used in [3] is given by

$$B = H e^{(1)} \wedge e^{(2)} = H R^2 \sin \bar{\theta} d\bar{\theta} d\bar{\phi} = d(-H R^2 \cos \bar{\theta} d\bar{\phi}), \quad (3.6)$$

where the local tetrads are given by

$$e^{(1)} = R d\bar{\theta}, \quad e^{(2)} = R \sin \bar{\theta} d\bar{\phi}, \quad e^{(3)} = R \cos \bar{\theta} d\bar{\psi}. \quad (3.7)$$

In order to show that (3.6) does not satisfy the second equation of motion (3.3), we split the inverse matrix  $\mathcal{E}^{ab}$  into two parts as follows

$$\mathcal{E}^{ab} = S^{ab} + J^{ab} \quad (3.8)$$

where  $S^{ab}$  is the symmetric while  $J^{ab}$  is the antisymmetric part of  $\mathcal{E}^{ab}$ . When evaluated on the ansatz (3.6) the antisymmetric part  $J^{ab}$  becomes

$$J^{\bar{\theta}\bar{\phi}} = -\frac{HR^2}{\sin \bar{\theta} \left( H^2 R^4 + \left( u - \frac{R^2}{4u} \right)^4 \right)} = -J^{\bar{\phi}\bar{\theta}}. \quad (3.9)$$

and hence the left hand side of the second equation of motion (3.3) becomes

$$\begin{aligned} \partial_a(\sqrt{-\mathcal{E}}(\mathcal{E}^{a\bar{\phi}} - \mathcal{E}^{\bar{\phi}a})) &= \partial_{\bar{\theta}}(\sqrt{-\mathcal{E}}(\mathcal{E}^{\bar{\theta}\bar{\phi}} - \mathcal{E}^{\bar{\phi}\bar{\theta}})) \\ &= -\frac{2HR^2}{H^2 R^4 + \left( u - \frac{R^2}{4u} \right)^4} \partial_{\bar{\theta}} \left( \frac{\sqrt{-\mathcal{E}}}{\sin \bar{\theta}} \right) \\ &= \frac{2HR^5 u}{\sqrt{H^2 R^4 + \left( u - \frac{R^2}{4u} \right)^4}} \sin \bar{\theta} \sin \theta \cos \theta \cos^3(\theta_3(u)) \\ &\quad \times \left( 1 - \frac{R^4}{16u^4} \right) \sqrt{1 + u^2 \theta_3'(u)^2} \\ &\neq 0. \end{aligned} \quad (3.10)$$

Hence in what follows, we focus on the ansatz (3.4) for the magnetic field which is based on spherical harmonics, and can be made to satisfy all equations of motion. As we will see the physical solutions for the brane embeddings are qualitatively very different from the results which were obtained in [3].

We also need to make an ansatz for the brane embedding. Since the magnetic field is turned on in the direction of the boundary  $S^3$ , we only need one transverse scalar to describe the shape of the D7-brane. While the external magnetic field introduced via (3.4) on the boundary sphere is obviously not constant, its norm, however, is. Moreover, it can be shown that our ansatz preserves an  $SO(3) \times SO(2)$  subgroup of the full  $SO(4)$  isometry group of the boundary  $S^3$ . Assuming that the scalar  $\chi$  preserves the same amount of symmetry, this then implies that it can depend only on the holographic direction  $u$ . Hence we make the ansatz for the scalar which field which depends only on the  $u$ -coordinate,

$$\chi = \chi(u), \quad \kappa = 0. \quad (3.11)$$



Substituting the ansatz (3.4) and (3.11) into the action one gets

$$\begin{aligned}
S = & -T_{D7} \frac{R^3}{2} \int d^8 \sigma \sin(\theta) \cos(\theta) \sin(\bar{\theta}) \cos(\bar{\theta}) \frac{u}{R} \left( 1 + \frac{R^2}{4u^2} \right) \\
& \times \sqrt{\left( (1 - \chi(u)^2) \left( 4 \left( 1 - \frac{R^2}{4u^2} \right)^2 R^2 + H'(u)^2 R^4 \right) + 4u^2 \left( 1 - \frac{R^2}{4u^2} \right)^2 R^2 \chi'(u)^2 \right)} \\
& \times \sqrt{\left( u^4 \left( 1 - \frac{R^2}{4u^2} \right)^4 + H(u)^2 R^4 \right) (1 - \chi(u)^2)} . \quad (3.12)
\end{aligned}$$

The equation of motion for  $\chi$  that follows from this action is given by

$$\begin{aligned}
0 = & \chi''(u) - \frac{4\chi(u)\chi'(u)^2}{\chi(u)^2 - 1} + \frac{3\chi(u) \left( 4R^2 u^4 H'(u)^2 + (R^2 - 4u^2)^2 \right)}{(R^2 u - 4u^3)^2} \\
& + \frac{\left( 256R^8 u^4 H(u)^2 + 12288R^4 u^8 H(u)^2 + (R^2 - 4u^2)^4 (3R^4 + 16R^2 u^2 + 80u^4) \right) \chi'(u)}{u(4u^2 - R^2)(R^2 + 4u^2)(256R^4 u^4 H(u)^2 + (R^2 - 4u^2)^4)} \\
& + \frac{\left( 1024R^6 u^8 H(u)^2 + 4(R^2 - 4u^2)^2 (3R^6 u^4 + 8R^4 u^6 + 48R^2 u^8) \right) H'(u)^2 \chi'(u)}{u(4u^2 - R^2)(R^2 + 4u^2)(256R^4 u^4 H(u)^2 + (R^2 - 4u^2)^4)} \\
& + \frac{4u \left( 128R^4 u^4 H(u)^2 (R^4 + 16u^4) + (R^2 - 4u^2)^4 (R^4 + 4R^2 u^2 + 16u^4) \right) \chi'(u)^3}{(R^2 - 4u^2)(R^2 + 4u^2)(\chi(u)^2 - 1)(256R^4 u^4 H(u)^2 + (R^2 - 4u^2)^4)} . \quad (3.13)
\end{aligned}$$

The equation of motion for the  $B$ -field, expressed in terms of the flux  $H$ , reads

$$\begin{aligned}
0 = & H''(u) - \frac{256R^4 u^4 H(u) H'(u)^2}{256R^4 u^4 H(u)^2 + (R^2 - 4u^2)^4} \\
& - \frac{4R^2 u^3 \left( 256R^4 u^4 H(u)^2 + (R^2 - 4u^2)^2 (3R^4 + 8R^2 u^2 + 48u^4) \right) H'(u)^3}{(R^2 - 4u^2)(R^2 + 4u^2)(256R^4 u^4 H(u)^2 + (R^2 - 4u^2)^4)} \\
& + \frac{64H(u) (R^3 - 4Ru^2)^2 (u^2 \chi'(u)^2 - \chi(u)^2 + 1)}{(\chi(u)^2 - 1)(256R^4 u^4 H(u)^2 + (R^2 - 4u^2)^4)} \\
& + \frac{\left( (R^2 - 4u^2)^4 (R^4 + 48u^4) - 256R^4 u^4 H(u)^2 (R^4 + 16R^2 u^2 - 16u^4) \right) H'(u)}{u(4u^2 - R^2)(R^2 + 4u^2)(256R^4 u^4 H(u)^2 + (R^2 - 4u^2)^4)} \\
& + \frac{4u \left( 128R^4 u^4 H(u)^2 (R^4 + 16u^4) + (R^2 - 4u^2)^4 (R^4 + 4R^2 u^2 + 16u^4) \right) H'(u) \chi'(u)^2}{(R^2 - 4u^2)(R^2 + 4u^2)(\chi(u)^2 - 1)(256R^4 u^4 H(u)^2 + (R^2 - 4u^2)^4)} . \quad (3.14)
\end{aligned}$$

These same equations can be obtained by first varying the action and then inserting the ansatz, as we have explicitly verified.

## 4 Solving the equations of motion

We now want to solve the equations of motion (3.14), (3.13) for the brane shape and worldvolume flux. As reviewed before, in the absence of flux there are two possible embeddings of the D7-brane, Minkowski and ball embeddings. We expect that these two classes will continue to exist, at least for small values of the magnetic field. We therefore impose the same type of boundary conditions on the brane shape as in the absence of the worldvolume flux, and then solve the equations including the magnetic field.

For Minkowski embeddings, we impose that the D7-brane caps off at some finite distance (IR “endpoint”)  $u = u_{\text{Mink}}$ . In other words, the  $S^3$  in  $S^5$  wrapped by the brane shrinks to zero size, so that  $\chi(u = u_{\text{Mink}}) = 1$ . In addition we require that there is no conical singularity present at the tip of the brane (as in [1]). This implies that the general expansion of the D7-brane near the tip is given by

$$\begin{aligned}\chi(u) &= 1 + \chi_{M1}(u - u_{\text{Mink}}) + \chi_{M2}(u - u_{\text{Mink}})^2 + O((u - u_{\text{Mink}})^3), \\ H(u) &= H_M + H_{M1}(u - u_{\text{Mink}}) + H_{M2}(u - u_{\text{Mink}})^2 + O((u - u_{\text{Mink}})^3),\end{aligned}\tag{4.1}$$

where  $\chi_{M1}, H_{M1}$  are long expressions of  $u_{\text{Mink}}, H_M$ .

For the ball embeddings, the D7-brane reaches all the way to the AdS origin where the  $S^3$  in  $AdS_5$  shrinks to zero size, while the  $S^3$  in  $S^5$  remains of finite size at that point. Since the magnetic field points in the direction of the shrinking  $S^3$  we have to require that at the origin of the  $AdS_5$  space the magnetic field vanishes. We also impose a Neumann boundary condition for the brane shape at the origin of the AdS space  $\chi'(u = u_{\text{ball}}) = 0$ , again similar to [1]. Putting all this together, we have for the general expansion of the ball brane near the AdS origin

$$\begin{aligned}\chi(u) &= \chi_{\text{ball}} - \frac{3}{16R^2} \left(-\frac{R}{2} + u\right)^2 (16 + H_{c2}^2) \chi_{\text{ball}} + O((u - R/2)^3), \\ H(u) &= \frac{H_{c2}}{R^2} \left(-\frac{R}{2} + u\right)^2 - 2\frac{H_{c2}}{R^3} \left(-\frac{R}{2} + u\right)^3 + O((u - R/2)^4),\end{aligned}\tag{4.2}$$

where  $\chi_{\text{ball}}$  parametrises the size of the  $S^3$  in  $S^5$  at the origin of the AdS space.

We also need the expansion of the scalar  $\chi$  and magnetic field  $H$  at infinity, in order to read off the physical parameters of the system. The general expansion of the

bulk fields near the AdS boundary is given by

$$\begin{aligned}\chi(u) &= \frac{m}{u} + \frac{c_1}{u^3} - \frac{mR^2}{2u^3} \log \frac{u}{R} + O(u^{-4}), \\ H(u) &= H_{\text{ext}} + \frac{M_{tz}}{u^2} - \frac{2H_{\text{ext}}R^2}{u^2} \log \frac{u}{R} + O(u^{-3}).\end{aligned}\tag{4.3}$$

In order to get rid of the divergent logarithmic terms, we need to renormalise the parameters in this expansion, following the holographic renormalisation procedure which was developed in [6]. Full details of this derivation are presented in [7]. One finds for the renormalised parameters

$$c = c_1 - \frac{mR^2}{2} \log \frac{m}{R}, \quad M = M_{tz} + H_{\text{ext}}R^2.\tag{4.4}$$

The physical parameters of the system are the bare “quark” mass  $m_q = m/2\pi\alpha'$  (i.e. the mass of the fermions in the hypermultiplet) and its condensate  $c$ . As the system is exposed to the nonconstant external magnetic field (3.4) with “amplitude”  $H_{\text{ext}}$ , a non-vanishing magnetisation  $M$  is present in the ground state. Our goal now is to understand the geometry of the branes as a function of the external magnetic field, and to determine how the magnetisation and the condensate vary as the external field is varied.

The equations of motion for the scalar  $\chi$  and magnetic field  $H$  are complicated, and in order to solve them we need to resort to numerical methods. We solve the equations directly by starting the numerical evolution from the origin (for ball branes) or the tip of the D7-brane (for Minkowski branes), as in [1]. However, as a cross check of our results, we have also used the more complicated shooting method which starts from the boundary of the AdS space and scans through the parameter space in order to find solutions that satisfy the boundary conditions at the origin or tip. While it is possible to perform a full numerical analysis in the  $u$ -coordinates (and we have solved the equations in this system as well), in order to have a numerical solution which covers the full AdS space (with no asymptotic cutoff), we present here the results in the compact coordinates (2.5), in which the origin of the AdS space is at  $z = 1$  and the boundary is at  $z = 0$ .

As said above, integrating outwards from the origin or tip of AdS is much simpler than shooting from the boundary. The main point is that since the regularity conditions for the behaviour of the brane at the origin or tip have already been built in to the expansions (4.2), (4.1), one always finds a physical solution for any value of the two free parameters (the position of the brane at the origin or tip, and the value of the magnetic field there). On the other hand, when shooting from infinity, one has to scan through

a four dimensional space of parameters while searching for a small two-dimensional subspace of solutions which behave in a regular fashion near the origin. The price one has to pay, however, when shooting from the origin is that, although the computation is simpler, the physical parameters can only be read off *after* the solutions have been constructed. So if one encounters a situation, as we will, that there appear forbidden regions in the physical parameter space, one cannot easily see what goes “wrong” with the solutions in this region of parameter space. For this reason we considered it essential to be able to reproduce the results using these two different methods, integrating from the origin/tip or shooting from the boundary. Some more technical comments on the techniques used to shoot from the boundary will be presented in section 4.1.

Solutions for the various shapes of D7-branes are plotted in figure 2. We also present the profile of the magnetic field for various values of the external parameter  $H_{\text{ext}}$ , see figure 3. For completeness, we also present the shapes and worldvolume magnetic field for various brane embeddings in the more familiar  $u$ -coordinates, see figures 4 and 5. However, note that in these coordinates one cannot numerically reach infinity, i.e. the boundary of AdS space, so all numerical computations are performed with some cutoff on the  $u$ -coordinate.

From the first plot in figure 2 we see that in the absence of the magnetic field both types of branes are “pulled” by gravity towards the origin of AdS space, i.e.  $z = 1$ . As the magnetic field is introduced, the probe branes first tend to be more flat (i.e. they fall less in the  $\chi$  direction) and then they bend away in the  $\chi$  direction as they get more and more “repelled” by the magnetic field. In other words, the magnetic field has an effect opposite from that of gravity. A similar kind of behaviour was observed before in the AdS space in Poincaré coordinates in [5, 8].

We also observe that as the magnetic field is increased, ball branes characterised by higher mass will start to disappear from the spectrum. In other words, if the bare quark mass is larger than some critical value  $\Delta m$ , then such ball branes cannot exist any longer (see figure 6). As a consequence, we see that a “gap” between the Minkowski branes phase (upper, blue) and ball brane phase (lower, red) starts to form. The  $y$ -axis on these plots is  $\chi/(2z)$ , i.e. it is proportional to the bare quark mass of the theory, while the horizontal axis labels  $z$ . We thus see that the gap between the two phases is characterised by a gap in the spectrum of *bare* quark masses.

As the magnetic field is increased, more and more ball branes disappear from the spectrum. When magnetic field reaches the “critical” value  $\hat{H}_1 \sim 3.98$ , all ball branes have disappeared from the spectrum and only Minkowski branes are present in the spectrum.

At the same time, the effect of the magnetic field on the Minkowski branes is to reduce the value for which the Minkowski brane with the smallest quark mass exists.

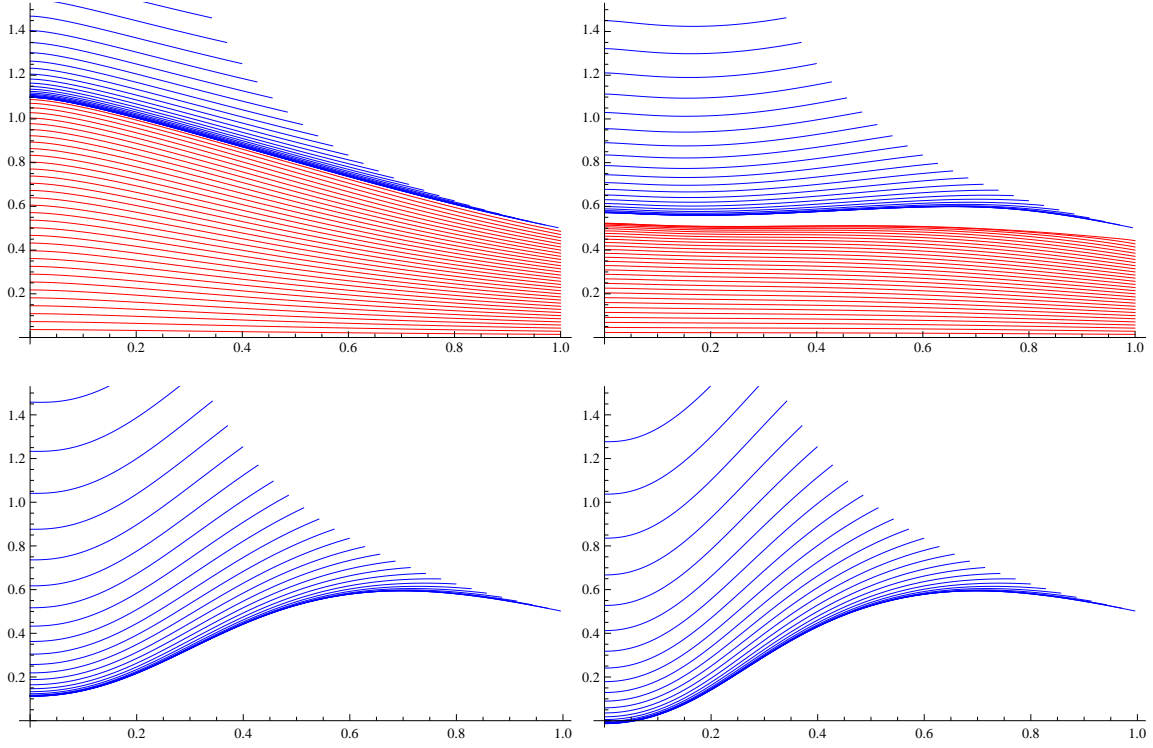


**Figure 2.** Brane shapes for D7 embeddings in the  $z$ -coordinate. From left to right and top to bottom the external magnetic field takes values  $H_{\text{ext}} = 0, 2, 4, 5$  respectively. Red is for ball embeddings where D7 reaches the AdS centre, while blue is for Minkowski embeddings where the D7 does not reach the AdS centre. The horizontal and vertical axes label  $z$  and  $\chi/(2z)$ . The quark mass of each embedding is proportional to the position of the brane on the vertical axis. The plots clearly show the development of a mass gap.

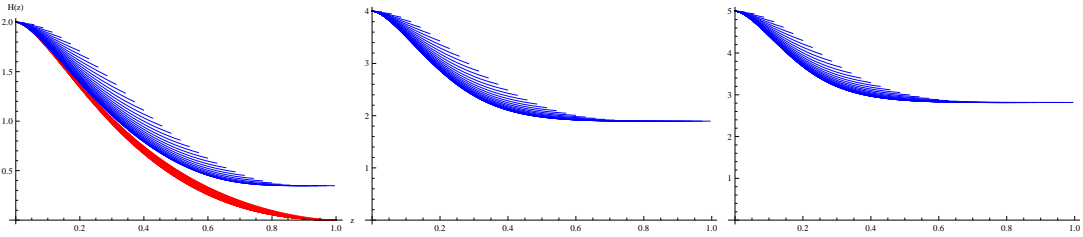


**Figure 3.** Plot of the profile  $H(z)$  for various brane embeddings. From left to right the external magnetic field takes values  $H_{\text{ext}} = 2, 4, 5$  respectively. Red is for ball embeddings where the D7-brane reaches the AdS centre. Blue is for Minkowski embeddings where the D7-brane does not reach the AdS centre.

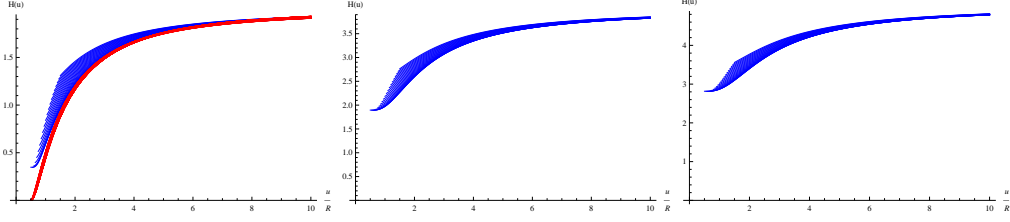


**Figure 4.** Plot of the profile  $H(u)$  for different branes embedding. From left to right and top to bottom shows the plot at fixed external magnetic field  $H_{\text{ext}} = 2, 4, 5$ , respectively. Red is for ball embedding where D7 reaches AdS centre. Blue is for Minkowski embedding where D7 does not reach AdS centre.

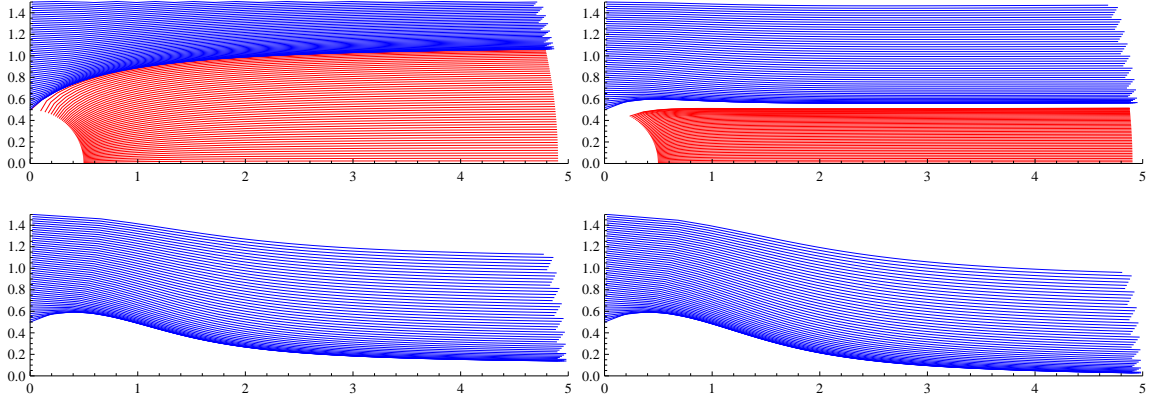


**Figure 5.** Plot of brane shapes for D7 embedding. From Left to Right and Top to Bottom shows the plot at fixed external magnetic field  $H_{\text{ext}} = 0, 2, 4, 5$ , respectively. Red is for Ball embedding where D7 reaches AdS centre. Blue is for Minkowski embedding where D7 does not reach AdS centre. The horizontal and vertical axes are  $u\sqrt{1-\chi^2}, u\chi$ . We see the development of mass gap as external magnetic field is increased roughly to  $H_{\text{ext}} = 4$ . The gap closes again around  $H_{\text{ext}} = 5$  where the lowest Minkowski embedding has zero quark mass.

As the ball branes disappear from the spectrum, at the same time the spectrum of the Minkowski branes is shifted towards lower values of the bare quark mass. As one increases the value of the magnetic field above  $\hat{H}_1$ , no ball branes are left in the spectrum, and the size of the gap (i.e. the non-allowed region for the mass) starts to decrease. When the magnetic field reaches  $\hat{H}_2 \sim 5$ , the gap closes, and for  $H > \hat{H}_2$  there is no gap. At this stage even the  $m = 0$  brane is Minkowski, and will not reach the origin of the AdS space; this thus spontaneously breaks the reflection symmetry of

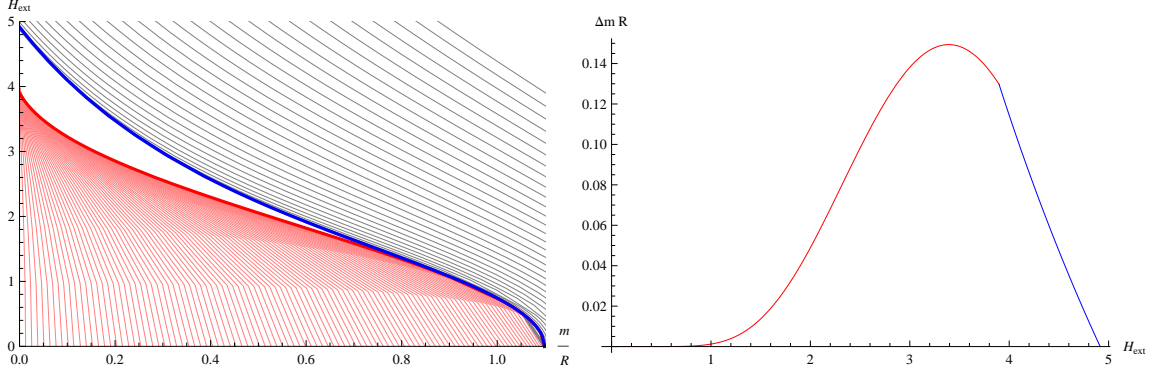


**Figure 6.** The panel on the left shows the possible values of  $H_{\text{ext}}$  and  $m$ . The red region corresponds to ball branes, while the grey region (above the blue line) corresponds to Minkowski branes, which are all uniquely specified given the values  $(H_{\text{ext}}, m)$ . The curves are just an artifact of the discrete steps which were used to scan the full parameter space. The panel on the right shows the behaviour of the “mass gap” in the full parameter space as a function of the external magnetic field. The gap begins to develop as soon as  $H_{\text{ext}} > 0$  and it closes again at  $H_{\text{ext}} = \hat{H}_2 \approx 5$ .

the space. The behaviour of the gap as a function of the external field is shown on the right hand side of figure 6. This is in qualitative agreement with the observation of [5], who have found, for embeddings in the background of a black hole in the Poincaré patch, that for large enough values of the external magnetic field no branes can fall into the black hole.

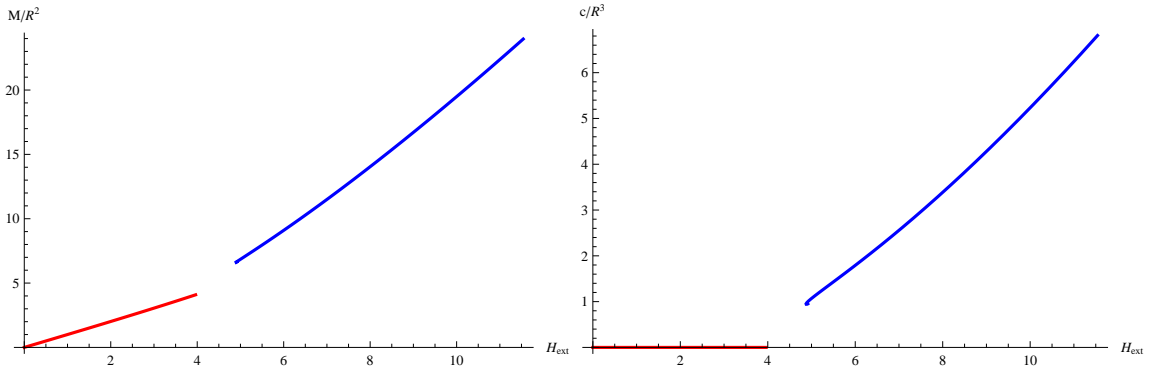


**Figure 7.** The behaviour of the “condensates”  $M(H_{\text{ext}})$  and  $c(H_{\text{ext}})$  for  $m = 0$  branes; see (4.4) for their definition in terms of the bare parameters  $c_1$  and  $M_{t\bar{z}}$ .

## 4.1 Comments on the numerical analysis

Constructing solutions by starting from the origin is straightforward. In order to ensure that the mass gap, which we first observed in the brane embeddings obtained with this method, is not due to an error in our Mathematica code, we have independently verified these solutions with an ODE solver built using [9]. This revealed no significant differences.

Constructing solutions by starting from the boundary at  $z = 0$  is considerably more challenging, as was already alluded to earlier. At the boundary we have four parameters at our disposal:  $m$ ,  $H_{\text{ext}}$  and  $c_1$  and  $M_{tz}$ . Since we are mostly interested in understanding the gap in  $m$  for a fixed value of  $H_{\text{ext}}$ , we proceed by fixing both these parameters and performing a two-dimensional search for solutions in the plane spanned by  $c_1$  and  $M_{tz}$ . One expects on general grounds that there will be a region in this plane for which the solutions  $\chi(z)$  and  $H(z)$  remain regular. Inside that region one then expects two curves, corresponding to solutions that satisfy one of the two boundary conditions at the origin (for ball branes) or at the turning point (for Minkowski branes). Physical solutions lie on the intersection point of these two curves (if it exists). However, an explicit analysis shows that the region of regular solutions is in fact already essentially (up to numerical errors) one-dimensional.

The two-dimensional scan for regular solutions is done with a multi-grid method. We start with a grid which, somewhat arbitrarily, spans  $-10 \leq c_1/R^3 \leq 10$  and  $-10 \leq M_{tz}/R^2 \leq 10$  with unit grid size in both parameters. We label the points on this grid by a number which describes how close the corresponding solutions are to being regular (described in more detail below). After this, we re-initialise the algorithm with a new and denser grid that contains a set of points for which this number is smallest. Interestingly we find that the set of regular solutions is essentially one-dimensional, and all solutions on this curve also satisfy one of the boundary conditions. Once we have found this curve, we then switch to an algorithm somewhat similar to the one in [10] to trace along the curve of regular solutions in the two-dimensional parameter space. We then either find a point on the curve where both boundary conditions hold, or no such point (and no physical solution).

When we are looking for ball solutions, the measure that describes how close we are to a physical brane solution is taken to be the distance to the boundary (in the  $z$  coordinate) at which either  $H'(z)$  or  $\theta'(z)$  diverges. If the solution remains smooth and reaches the origin, this distance is zero. Such solutions can still have  $H(z = 1) \neq 0$ , so we then trace the curve of physical solutions and determine the value  $H(z = 1)$  on each point of this curve. A physical solution exists if there is a point in parameter space for which this value vanishes. A representative case is displayed in figure 8.



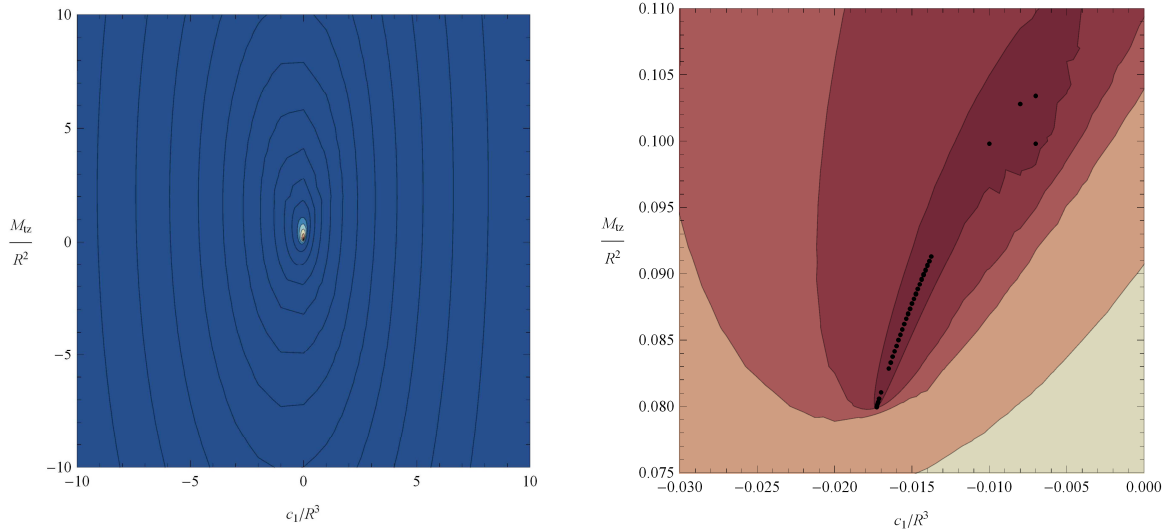


**Figure 8.** Typical search for a ball brane solution at  $(m/R, H_{\text{ext}}) = (0.4, 1)$ , which is known to exist from the shooting procedure from the origin (see the left panel of figure 6). The left plot shows a steep well of solutions which get close to a regular solution only in the neighbourhood of  $(c_1/R^3, M_{tz}/R^2) \approx (-0.015, 0.09)$ . The right plot shows a zoomed region, with black dots representing regular solutions, which also satisfy  $\theta'(z=1) = 0$ . The point at the bottom end of this curve has  $H(z=1) = 0$ . Red and blue colours represent small and large values of the deviation from regularity, respectively.

For the construction of Minkowski solutions, we first determine the location  $z = z_{\min}$  at which either  $\theta'(z)$  diverges, or for which  $H'(z)$  diverges or  $\theta(z) < 0$ . Closeness to a physical solution is then measured by the deviation of  $\sin \theta(z_{\min})$  from  $\pi/2$ . Recursing with a finer grid then eventually again leads to a curve of regular solutions, on which there is at most one point for which both boundary conditions hold.

## 5 Understanding the mass gap and behaviour of ball branes

Our findings from the previous section are interesting, although unusual, as they seem to impose a constraint on the *bare* quark masses, i.e. an “external” parameter of the system. In the present section we would therefore like to see if we can understand the origin of the gap which the magnetic field has introduced in the mass spectrum. We will do this by following what is happening with branes which, in the absence of a magnetic field, have two separated phases.

We would also like to see more explicitly how the ball branes disappear from the spectrum as the magnetic field is increased, and to better understand the nature of the maximal value of the magnetic field  $\hat{H}_2$ , beyond which no ball brane is present in

the spectrum. We will do this by following what is happening with the equatorial ball brane, which is the simplest of all the ball branes and the last to disappear when the external field reaches its maximal value.

### 5.1 Appearance of the gap: disappearance of critical branes

In the absence of a magnetic field the two observed phases are separated by a critical brane, i.e. a brane which satisfies both the Minkowski and the ball brane boundary conditions. So to understand better the origin of the gap, we will now show *analytically* that these branes are no longer possible as soon as a magnetic field is introduced.

The boundary conditions which are satisfied by critical branes are given by

$$\chi\left(u = \frac{R}{2}\right) = 1, \quad H\left(u = \frac{R}{2}\right) = 0, \quad (5.1)$$

since both  $S^3$  in  $AdS_5$  and  $S^3$  in  $S^5$  shrink to zero size for these branes. Therefore the most general expansion satisfying both of these conditions is given by

$$\begin{aligned} \chi(u) &= 1 + \chi_1(u - R/2) + \chi_2(u - R/2)^2 + O((u - R/2)^3), \\ H(u) &= H_{c1}(u - R/2) + H_{c2}(u - R/2)^2 + O((u - R/2)^3). \end{aligned} \quad (5.2)$$

By plugging these into the equations of motion, and expanding near the origin to the second order, one obtains two analytic solutions. For one of the solutions the variable  $\chi$  is manifestly larger than one, and as such is unacceptable, bearing in mind that  $\chi$  is the cosine of an angular variable. Another solution is given by

$$\begin{aligned} \chi(u) &= 1 - 2(u - R/2)^2 + 4(u - R/2)^3 - \frac{52}{15}(u - R/2)^4 + O((u - R/2)^5), \\ H(u) &= O((u - R/2)^5). \end{aligned} \quad (5.3)$$

So we see that the requirement of an analytic solutions of the equations of motion near the AdS origin implies that branes with a critical embedding are possible only if there is no magnetic field turned on (we have verified  $H(u)$  vanishes to much higher order). This fact is suggestive of the formation of a gap between the two phases, at least in the interior of the AdS space. Of course, there is a logical possibility that another type of phase appears in the gap, which is characterised by boundary conditions or symmetries which are different from the ones we have assumed so far, and were therefore missed in the analysis above. We will shed some more light on this point when we analyse the fluctuations of the ball and Minkowski branes in section 6.

## 5.2 Behaviour of the equatorial brane and maximal value of magnetic field

In order to get a better understanding of the disappearance of ball branes, and of the critical magnetic field  $\hat{H}_1$ , we will now focus our analysis on the simplest of ball branes, the equatorial brane. As it has the smallest bare mass, this ball brane is the last one to disappear from the spectrum.

The equatorial brane is the simplest ball brane which exists, and is characterised by  $m = 0$  and  $\chi = 0$ . In the absence of the external field, this brane is “flat” i.e. it has a worldvolume metric  $\text{AdS}_5 \times S^3$ , a submanifold of vanishing extrinsic curvature. As the magnetic field is turned on, the shape of this brane does not change, which is guaranteed by symmetry arguments, and easily confirmed by equations of motion. However, one still needs to solve the equations of motion for the magnetic field on the brane worldvolume.

The action for the magnetic field is relatively simple and given by

$$S = -T_{D7} \frac{R^7}{16} \int d^8 \sigma \frac{1}{z^5} (z^2 + 1) \sin \theta \cos \theta \sin \bar{\theta} \cos \bar{\theta} \times \sqrt{(16z^4 H(z)^2 + (z^2 - 1)^4) (z^4 H'(z)^2 + (z^2 - 1)^2)}, \quad (5.4)$$

while the equations of motion are

$$\begin{aligned} H''(z) - \frac{16z^4 H(z) H'(z)^2}{16z^4 H(z)^2 + (z^2 - 1)^4} - \frac{16(z^2 - 1)^2 H(z)}{R^2 (16z^4 H(z)^2 + (z^2 - 1)^4)} \\ + \frac{(16(z^4 - 4z^2 - 1) z^4 H(z)^2 + (z^2 - 1)^4 (3z^4 + 1)) H'(z)}{16(z^4 - 1) z^5 H(z)^2 + (z^2 - 1)^5 (z^2 + 1) z} \\ + \frac{R^2 z^3 (16z^4 H(z)^2 + (z^2 - 1)^2 (3z^4 + 2z^2 + 3)) H'(z)^3}{16z^4 (z^4 - 1) H(z)^2 + (z^2 + 1) (z^2 - 1)^5} = 0. \end{aligned} \quad (5.5)$$

These equations still have to be solved numerically. However, we are now dealing only with two free parameters  $(H_{\text{ext}}, M)$ . So we can solve them by shooting either from infinity or from the origin, and in that way cross check our findings.

Observe that the action for equatorial brane (5.4) is always real for all values of the magnetic field. In other words, the reality condition on the action does not imply the existence of a maximal value of the external magnetic field, but this will have to come out from solving equations.

For generic values of the parameters  $(H_{\text{ext}}, M_{tz})$  at infinity, the magnetic field of the solution at the origin of the AdS space has a non-vanishing value, or its derivative

blow up. However, for the points on the green line of figure (5.2) the magnetic field satisfies the required boundary condition at the origin and it is regular everywhere. We see that this green line of physical solutions is *part* of the borderline between the red region (where the magnetic field has non-vanishing value at the origin) and the blue region (where the derivative of the magnetic field blows up in the interior of AdS space).

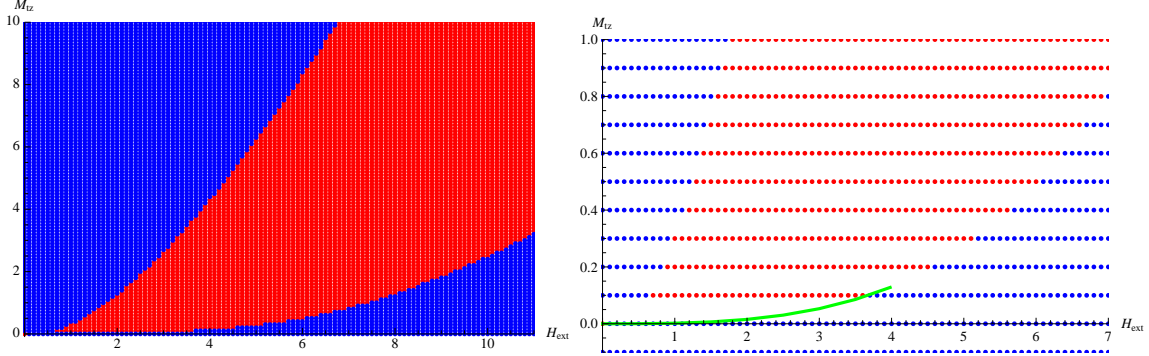


**Figure 9.** The plot shows the  $(H_{\text{ext}}, M_{tz})$  parameter space. In the red (middle) region, the value of the magnetic field at the origin is finite, but non-vanishing. In the blue (surrounding) regions the derivative of the magnetic field blows up as one approaches the origin of the AdS space. The physical solutions are located on the borderline, between the two regions, as shown in the plot on the right hand side (green curve).

By looking at right hand side plot of figure (5.2) we see that the green line of physical solutions stops for some “critical” value of the external field  $H_{\text{ext}} = \hat{H}_1 \approx 3.98$ . This signals that the equatorial Minkowski brane does not exist for a value of magnetic field which is larger than the value  $\hat{H}_1$ .

## 6 Fluctuation analysis and investigation of the gap

The analysis in the previous section suggests that the magnetic field introduces a gap in the spectrum and leads to the ball branes disappearing from the spectrum. However, there is a possibility that the branes which were analysed in the previous sections were not general enough, and that the appearance of the gap is a consequence of the fact that our ansatz was not general enough.

Therefore, in order to gain some insight into this question, it would as a first step be useful to understand the stability of the constructed branes under small fluctuations. In particular, we would like to understand the stability of branes near the gap. In the

present section we therefore initiate an analysis of the stability of branes near the gap, and discover an instability of the branes under the fluctuations of the transverse scalar mode. We then try to use this knowledge to shed some light on the potential branes which could fill out the gap.

### 6.1 Stability analysis of the branes

The stability analysis of a generic ball or Minkowski brane proves to be a very challenging numerical problem. The reason is that, to start with, all branes are known only numerically (except for the equatorial brane). In addition, for a generic brane, the transverse scalars and vector modes mix. The fluctuation analysis in [3] was done with a background magnetic field which does not satisfy the equations of motion (as already discussed in the section 3.1). Moreover, instead of first deriving the equations of motion for fluctuations and then plugging in the ansatz for the fluctuations, the authors of [3] inserted the fluctuation ansatz directly into the action, thus failing to check if the ansatz for the fluctuations is consistent with full equations of motion. Following the full path of first deriving equations of motion for the arbitrary brane near the gap is very involved, both analytically and numerically, as unfortunately the analysis does not seem to simplify near the gap. Fortunately, the analysis for the equatorial brane, which reaches the gap for  $H_{\text{ext}} \sim 3.98$ , is much simpler, and can be done in full generality. For this brane, the shape is simple and known explicitly. So in what follows we will focus on the equatorial brane, for a generic value of the magnetic field.

When studying the fluctuations around the configurations constructed in the previous sections, we will need the Wess-Zumino term in addition to the DBI action,

$$S_{\text{WZ}} = \frac{1}{2} T_{\text{D}7} (2\pi\alpha')^2 \int P[C_4] \wedge F \wedge F + \frac{1}{2} T_{\text{D}7} \int P[C_4] \wedge P[B] \wedge P[B] \\ + T_{\text{D}7} 2\pi\alpha' \int P[C_4] \wedge P[B] \wedge F, \quad (6.1)$$

where  $C_4$  is a 4-form gauge field with self-dual field strength  $F_5$  given by

$$F_5 = \frac{4}{R} (\text{Vol}(\text{AdS}_5) + \text{Vol}(S^5)) . \quad (6.2)$$

The equations of motion following from the full action are given by

$$\partial_a (\sqrt{-\mathcal{E}} (\mathcal{E}^{ab} - \mathcal{E}^{ba})) = -\frac{1}{5!} F_{a_1 a_2 a_3 a_4 a_5} \mathcal{F}_{a_6 a_7} \tilde{\epsilon}^{a_1 \dots a_7 b} \quad (6.3)$$

and

$$\begin{aligned}
& -\frac{1}{4 \cdot 4!} \tilde{\epsilon}^{a_1 \dots a_8} F_{\rho a_1 a_2 a_3 a_4} \mathcal{F}_{a_5 a_6} \mathcal{F}_{a_7 a_8} = \partial_b \left( \sqrt{-\mathcal{E}} (\mathcal{E}^{ba} + \mathcal{E}^{ab}) \right) G_{\nu\rho} \partial_a x^\nu \\
& + 2\sqrt{-\mathcal{E}} \mathcal{E}^{ba} \left( G_{\nu\rho} \partial_b \partial_a x^\nu + \frac{1}{2} (\partial_\mu G_{\rho\nu} - \partial_\rho G_{\mu\nu} + \partial_\nu G_{\mu\rho} \partial_a x^\mu \partial_b x^\nu) \right), \quad (6.4)
\end{aligned}$$

where  $\mathcal{F} = P[B] + 2\pi\alpha' F$ . Greek indices are spacetime indices while Roman indices are worldvolume indices. For the spacetime fields having worldvolume indices, it is understood that the fields are pulled back to the worldvolume.

Recall that the equatorial brane is specified by

$$\chi = 0, \quad \kappa = 0, \quad (6.5)$$

together with

$$\begin{aligned}
B = \frac{1}{2} H'(u) R^2 (\sin^2 \bar{\theta} du d\bar{\phi} + \cos^2 \bar{\theta} du d\bar{\psi}) \\
+ H(u) R^2 \sin \bar{\theta} \cos \bar{\theta} (d\bar{\theta} d\bar{\phi} - d\bar{\theta} d\bar{\psi}). \quad (6.6)
\end{aligned}$$

The fluctuations around the equatorial brane consist of scalars which are transverse to the brane worldvolume (these are not charged under the  $SO(4)$  isometry group of the  $S^3 \in S^5$  which is wrapped by the D7-brane), vector fluctuations in the direction of  $S^3 \in S^5$  (which are dual to scalars from the field theory point, we call these “charged scalars”) and vector fluctuations of the gauge field in the non-compact directions of the probe brane.

In order to study charged scalar fluctuations, we make the following ansatz,

$$\delta A_i = e^{-i\omega t} a_{\omega, \bar{l}, l, s}(u) Y^{\bar{l}}(\bar{\Omega}_3) Y_i^{l, s}(\Omega_3), \quad (6.7)$$

where  $Y^{\bar{l}}(\bar{\Omega}_3)$  are spherical harmonics,  $Y_i^{l, s}$  are vector spherical harmonics, with  $l, \bar{l}$  being integer and  $s = \pm 1$ . From the previous analyses in [4, 11], it is known that the mode with  $l = 1, s = -1, \bar{l} = 0$  has the lowest energy in the absence of a magnetic field. Since we do not expect modes to cross when the magnetic field is turned on, if there is an instability it will first show up in this mode of fluctuations. Therefore, in what follows we will focus on this fluctuation mode. The ansatz then becomes explicitly,

$$\delta A = a(t, u) (\sin^2 \theta d\phi + \cos^2 \theta d\psi), \quad a(t, u) = e^{-i\omega t} a(u). \quad (6.8)$$

The equation of motion for the charged scalar fluctuation  $a(u, t)$  is

$$a''(u) + \frac{\partial_u (\sqrt{-e} e^{uu})}{\sqrt{-e} e^{uu}} a'(u) + \frac{1}{e^{uu}} \left( \frac{4}{R^2} - e^{tt} \omega^2 \right) a(u) - \frac{2}{R^2} \left( 4g_{uu} + R^4 H'(u)^2 g^{33} - 4 \sqrt{\frac{g_{uu} e^{33}}{e^{uu} g^{33}}} \right) a(u) = 0. \quad (6.9)$$

This equation is very similar to the equations obtained in [4] for the analysis of the ground state of  $N = 2$  theory on  $S^3$  in the presence of an isospin chemical potential. The equation is solved by putting it into Schrödinger form. For all the technical details, we refer the reader to [4].

Solving the equations of motion for the fluctuations determines the frequencies of the fluctuations as functions of the external magnetic field. We impose the same boundary conditions for fluctuations as for the brane around which the fluctuations are excited. The solutions of the equations are labelled by an ‘ $n$ ’, a new integer quantum number. Figure 10 shows the frequencies of the first three modes  $n = 1, 2, 3$ . We see that despite the fact that the frequencies for the equatorial ball brane decrease as the external field increases, they remain positive even when all ball branes disappear. A similar analysis can be performed for non-vanishing quark masses, and a similar behaviour is observed for all other branes as shown in figure 11. We thus see no signs of instability under the fluctuations in the direction of the maximal  $S^3 \in S^5$ .

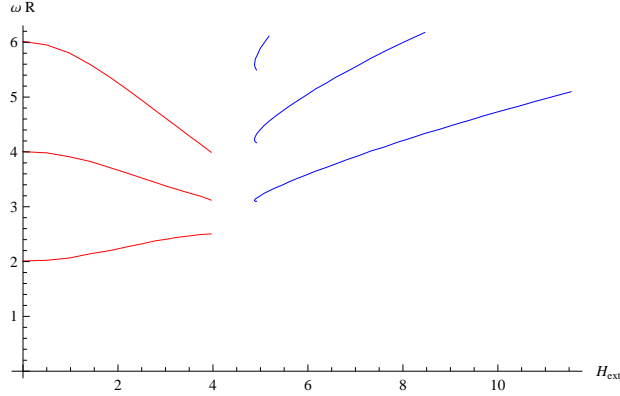


**Figure 10.** The first three normal modes of the charged scalar fluctuation (6.9) for fixed  $m = 0$ , as a function of the external magnetic field. Red shows the plot for ball embeddings while blue shows the plot for Minkowski embeddings.

Next we turn to the analysis of vector fluctuations in the direction of the AdS part of the brane worldvolume. This analysis is similar to the previous analysis of the

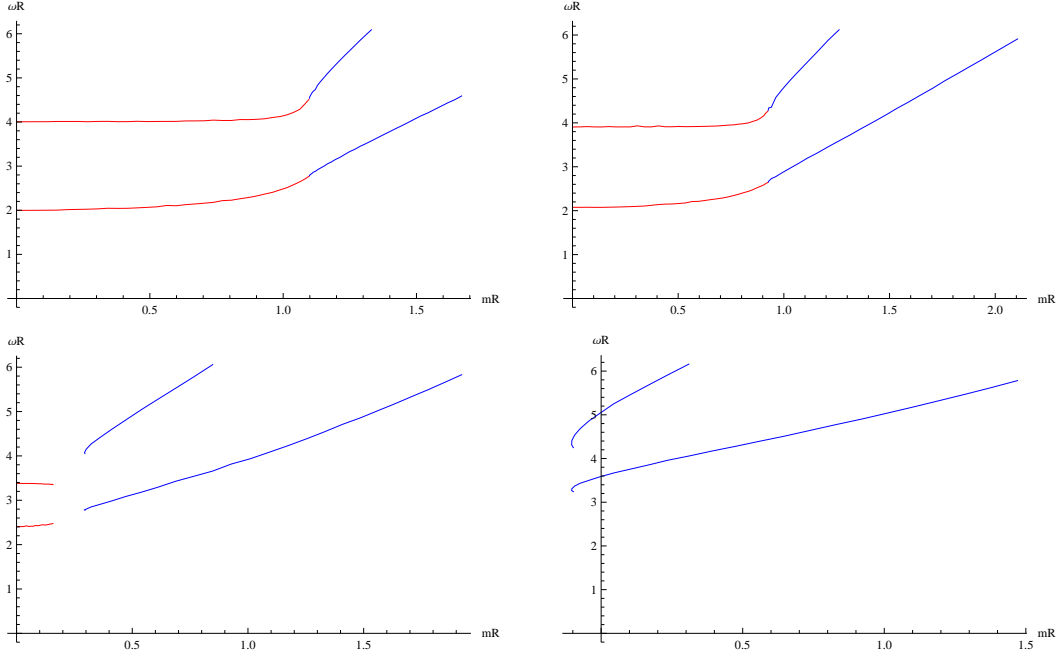


**Figure 11.** The first two normal modes of the charged scalar fluctuation (6.9) for fixed external magnetic field but varying quark mass. From left to right and top to bottom,  $H_{\text{ext}} = 0, 1, 3, 6$ , respectively. Red shows the plot for ball embeddings while blue shows the plot for Minkowski embeddings.

charged scalar, except that because the magnetic field is non-vanishing in the same directions as those in which we fluctuate (i.e. the  $\bar{S}^3 \in AdS_5$ ) the energy levels will in general split. Therefore, the magnetic quantum numbers should be also taken into account, so that one is in general dealing with  $Y^{l, m_1, m_2, s}$ . The general ansatz we make is

$$\delta A_i = e^{-i\omega t} a_{\omega, \bar{l}, \bar{m}_1, \bar{m}_2, \bar{s}}(u) \bar{Y}_i^{\bar{l}, \bar{m}_1, \bar{m}_2, \bar{s}}(\bar{\Omega}_3). \quad (6.10)$$

While we have performed the analysis for general  $m_1, m_2$  it turns out that  $(\bar{l}, \bar{m}_1, \bar{m}_2, \bar{s}) = (1, 0, 0, -1)$  is the lowest mode. The ansatz for the fluctuation given previously simplifies for the lowest lying mode to

$$\delta \bar{A} = \bar{a}(t, u) (\sin^2 \bar{\theta} d\bar{\phi} + \cos^2 \bar{\theta} d\bar{\psi}), \quad \bar{a}(u, t) = e^{-i\omega t} \bar{a}(u). \quad (6.11)$$



The equation of motion for the vector fluctuation  $\bar{a}(u, t)$  is

$$\begin{aligned} \bar{a}''(u) + \frac{\partial_u(\sqrt{-e}(e^{uu})^2 g_{uu} g^{33})}{\sqrt{-e}(e^{uu})^2 g_{uu} g^{33}} \bar{a}'(u) - \frac{\omega^2 e^{tt} + 4e^{33}}{e^{uu}} \bar{a}(u) \\ + \left( 2H'(u) \frac{\partial_u g^{33}}{g_{uu} (g^{33})^2} + 8H(u) \right) H(u) R^4 (e^{33})^2 \frac{g^{33}}{e^{uu}} \bar{a}(u) = 0. \end{aligned} \quad (6.12)$$

After an analysis similar to the one for the charged scalar, we get the frequencies as a function of the external field. These are presented in figure 12. We again observe that all modes stay positive definite, even if the magnetic field exceeds its critical value.

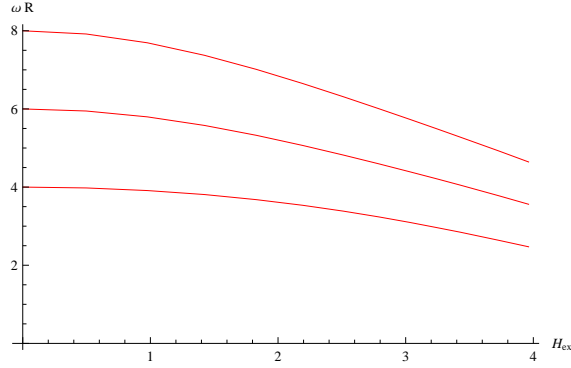


**Figure 12.** First three normal modes of the vector fluctuation (6.12) for the equatorial embedding  $m = 0$  as a function of the external field.

Let us finally turn to the scalar fluctuations. We focus on the equatorial embedding of the D7-brane. It is convenient to introduce coordinates on  $S^5$  as

$$w_1 = R \sin \theta \cos \phi \quad w_2 = R \sin \theta \sin \phi, \quad (6.13)$$

so that the metric on  $S^5$  becomes

$$ds_5^2 = \left( 1 - \frac{w_1^2 + w_2^2}{R^2} \right) d\Omega_3^2 + \frac{1}{1 - \frac{w_1^2 + w_2^2}{R^2}} \left( dw_1^2 + dw_2^2 - \left( \frac{w_2}{R} dw_1 - \frac{w_1}{R} dw_2 \right)^2 \right). \quad (6.14)$$

The embedding of the equatorial brane is given by

$$w_1 = w_2 = 0. \quad (6.15)$$

Hence, we make the following ansatz for the fluctuations,

$$\delta w_\mu = 2\pi\alpha' \Psi_\mu(u), \quad \mu = 1, 2. \quad (6.16)$$

The fluctuation equations are symmetric with respect to  $w_1$  and  $w_2$ , and moreover, it is consistent to set either of the two scalars to zero value. So we choose the following ansatz for the fluctuations

$$\Psi_1 = \Psi(u)e^{-i\omega t}, \quad \Psi_2 = 0. \quad (6.17)$$

Substituting this ansatz into the equations of motion, and linearising in the fields, one obtains the equation governing the dynamics of  $\Psi$ ,

$$\partial_u^2 \Psi(u) + \frac{\partial_u (\sqrt{-e} e^{uu})}{\sqrt{-e} e^{uu}} \partial_u \Psi(u) + \frac{1}{e^{uu}} \left( \frac{3}{R^2} - e^{tt} \omega^2 \right) \Psi(u) = 0. \quad (6.18)$$

where

$$\begin{aligned} \sqrt{-e} &= \frac{(R^2 + 4u^2) \sqrt{\left( 256R^4 u^4 H(u)^2 + (R^2 - 4u^2)^4 \right) \left( 4R^2 u^4 H'(u)^2 + (R^2 - 4u^2)^2 \right)}}{u^5}, \\ e^{uu} &= \frac{(R^2 u - 4u^3)^2}{4R^4 u^4 H'(u)^2 + (R^3 - 4Ru^2)^2}, \\ e^{tt} &= -\frac{16R^2 u^2}{(R^2 + 4u^2)^2}. \end{aligned} \quad (6.19)$$

By solving this equation we get the frequencies as functions of the external magnetic field and  $n$ , a new quantum number. These functions are shown in figure 13 for the first two lightest modes. We see that for large enough value of the magnetic field,  $H \sim 3.98$ , the lightest scalar mode becomes unstable. The value for which this happens is exactly the same as the value for which the equatorial ball brane disappears from the spectrum. So this perturbative analysis is consistent with our previous analysis, as it suggests that the real ground state for  $H > 3.98$  is no longer a ball brane.

## 6.2 Investigating the gap

An unusual feature of the gap which was discovered in the first part of the paper is that it introduces restrictions on the bare parameters of the theory. The gap in the spectrum forbids certain values of the bare quark masses, depending on the value of the external field. While this is in principle possible, we would like to eliminate the possibility that the presence of the gap is due to missed states with a different symmetry, which we have not allowed for in our analysis so far. While we do not yet have a conclusive answer to this question, we will present here our attempts to understand if there are additional states present in the “gap” part of the spectrum.

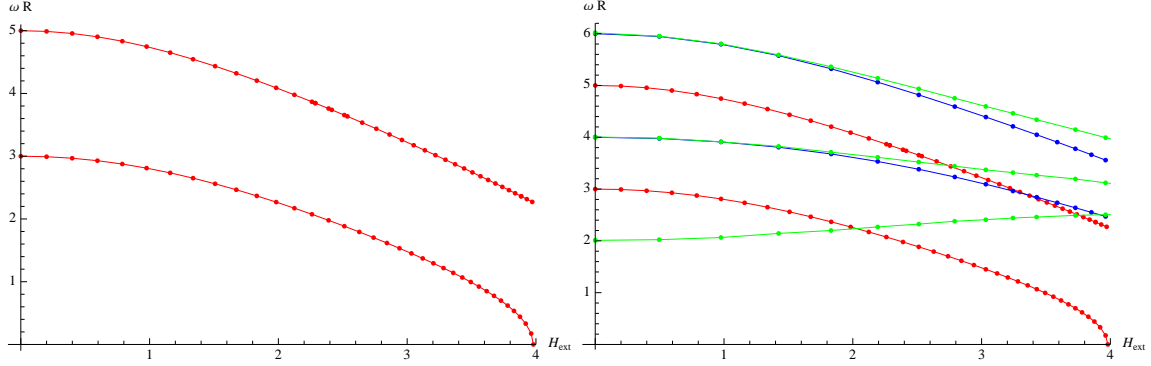


**Figure 13.** The panel on the left shows the first two normal modes of the scalar fluctuation (6.18) for the equatorial embedding  $m = 0$  but varying external magnetic field. The panel on the right shows these modes together with the charged scalar modes of figure 10 (green) and the vector modes of figure 12 (blue) plotted together. We see that the magnetic field makes the scalar fluctuation unstable.

One observation which we make is that if one relaxes the condition that the magnetic field has to vanish at the origin of the AdS space, then the gap can be filled completely with ball branes. Of course, these branes are unphysical as the magnetic field is non-vanishing in the direction of the  $S^3$  which shrinks to zero size at the origin of  $\text{AdS}_5$ . However, perhaps there is a way in which this kind of singular behaviour could be resolved by “blowing up” the shrinking  $S^3$ . We will leave this line of investigation for later and focus on an alternative route here.

The analysis of the fluctuations from the previous section suggests that branes near the gap are unstable under transverse scalar fluctuations. This suggests that near the branes which are at the edge of the gap, there could be a new, nearby ground state, which has less symmetry than either ball or Minkowski branes. In particular, since the unstable fluctuation breaks the  $\bar{SO}(4)$  symmetry preserved by ball and Minkowski branes, we expect that the new ground state should also break this symmetry. Making a general ansatz for the transverse scalar  $\chi$ , where it depends on all coordinates of the  $\bar{S}^3 \in \text{AdS}_5$ , gives a very complicated set of equations which we do not know how to analyse in full generality. Therefore, we will make the simplifying assumption that the real ground state is infinitesimally close to the equatorial brane, and use this to attempt to construct the new ground state perturbatively. A similar analysis was made (for a different model) in [12], who constructed the Abrikosov lattice in a holographic framework. The perturbative parameter is the distance from the critical magnetic field

for which the gap appears,

$$\Delta = \frac{H_{\text{ext}} - \hat{H}_1}{\hat{H}_1} \quad (6.20)$$

where  $\hat{H}_1 = 3.98$  for the equatorial brane.

We make the following ansatz

$$\begin{aligned} \delta\chi(u, \bar{\theta}, \bar{\phi}, \bar{\psi}) &= \Delta\chi_1(u, \bar{\theta}, \bar{\phi}, \bar{\psi}) + \Delta^3\chi_3(u, \bar{\theta}, \bar{\phi}, \bar{\psi}) + O(\Delta^5) \\ \delta\Lambda &= \Delta^2\Lambda_2 + \Delta^4\Lambda_4 + O(\Delta^6), \quad \delta B = d\delta\Lambda \end{aligned} \quad (6.21)$$

Here, alternating of the powers of the expansion in  $\delta\chi$  and  $\delta\Lambda$  is motivated by [12] and in turn by the original paper [13]. Plugging this ansatz into the equations of motion we can solve the equations order by order. We omit the details of this lengthy analysis here, but the upshot is that at third order in perturbation theory the equation for  $\chi_3$  does not seem to have a physical solution.

While this attempt does not seem to lead to a new ground state, we still believe that making some modifications of this approach will work. In particular, relaxing the alternating powers in the expansion (6.21) may help to resolve the issues which we observed. It may also be necessary to turn on a non-abelian component of the worldvolume gauge field, as was done in [12]. We intend to address these issues in future work.

## References

- [1] A. Karch and A. O'Bannon, *Chiral transition of  $N = 4$  super Yang-Mills with flavor on a 3-sphere*, *Phys. Rev.* **D74** (2006) 085033, [[hep-th/0605120](#)].
- [2] A. Karch, A. O'Bannon, and L. G. Yaffe, *Critical exponents from AdS/CFT with flavor*, *JHEP* **09** (2009) 042, [[arXiv:0906.4959](#)].
- [3] V. G. Filev and M. Ihl, *Flavoured large- $N$  gauge theory on a compact space with an external magnetic field*, *JHEP* **1301** (2013) 130, [[arXiv:1211.1164](#)].
- [4] S. Chunlen, K. Peeters, P. Vanichchapongjaroen, and M. Zamaklar, *Instability of  $N = 2$  gauge theory in compact space with an isospin chemical potential*, *JHEP* **1301** (2013) 035, [[arXiv:1210.6188](#)].
- [5] J. Erdmenger, R. Meyer, and J. P. Shock, *AdS/CFT with flavour in electric and magnetic Kalb-Ramond fields*, *JHEP* **0712** (2007) 091, [[arXiv:0709.1551](#)].
- [6] A. Karch, A. O'Bannon, and K. Skenderis, *Holographic renormalization of probe D-branes in AdS/CFT*, *JHEP* **0604** (2006) 015, [[hep-th/0512125](#)].
- [7] P. Vanichchapongjaroen, *Branes and Applications in String Theory and M-theory*. PhD thesis, Durham University, 2014.
- [8] V. G. Filev, C. V. Johnson, R. Rashkov, and K. Viswanathan, *Flavoured large- $N$  gauge theory in an external magnetic field*, *JHEP* **0710** (2007) 019, [[hep-th/0701001](#)].
- [9] K. Ahnert and M. Mulansky, *Odeint - solving ordinary differential equations in C++*, [1110.3397](#). <http://www.odeint.com>.
- [10] A. Ballon-Bayona, K. Peeters, and M. Zamaklar, *A chiral magnetic spiral in the holographic Sakai-Sugimoto model*, *JHEP* **1211** (2012) 164, [[arXiv:1209.1953](#)].
- [11] J. Erdmenger and V. Filev, *Mesons from global Anti-de Sitter space*, *JHEP* **1101** (2011) 119, [[arXiv:1012.0496](#)].
- [12] Y.-Y. Bu, J. Erdmenger, J. P. Shock, and M. Strydom, *Magnetic field induced lattice ground states from holography*, *JHEP* **1303** (2013) 165, [[arXiv:1210.6669](#)].
- [13] A. Abrikosov, *On the Magnetic properties of superconductors of the second group*, *Sov.Phys.JETP* **5** (1957) 1174–1182.